

$N(nPr)_4[B_5O_6(OH)_4][B(OH)_3]_2$ and $N(nBu)_4[B_5O_6(OH)_4][B(OH)_3]_2$: Clathrates with a Diamondoid Arrangement of Hydrogen-Bonded Pentaborate Anions

CLEMENS C. FREYHARDT, MICHAEL WIEBCKE* and
JÜRGEN FELSCHE

Faculty of Chemistry, University of Konstanz, P.O. Box 5560, 78434 Konstanz, Germany

and

GÜNTER ENGELHARDT

Institute of Chemical Technology I, University of Stuttgart, Pfaffenwaldring 55, 70550 Stuttgart, Germany

(Received: 21 February 1994; in final form: 14 June 1994)

Abstract. Single-crystal X-ray structure analyses of $N(nPr)_4[B_5O_6(OH)_4][B(OH)_3]_2$, **1**, and $N(nBu)_4[B_5O_6(OH)_4][B(OH)_3]_2$, **2**, reveal that these materials are novel clathrates, the isotypic host structures of which are three-dimensional assemblies of hydrogen-bonded $[B_5O_6(OH)_4]^-$ ions and $B(OH)_3$ molecules. The assembly of only the pentaborate anions is a distorted (i.e., along [102] elongated) four-connected diamond-related network. The $N(nPr)_4^+$ and $N(nBu)_4^+$ ions are trapped within the complex three-dimensional channel systems of the host frameworks. Both **1** and **2** crystallize monoclinically with space group $P2_1/c$ and $Z = 4$. The cell constants are: **1**: $a = 13.592(5)$, $b = 12.082(2)$, $c = 17.355(6)$ Å, $\beta = 106.60(2)^\circ$ (298 K); **2**: $a = 13.874(3)$, $b = 12.585(1)$, $c = 17.588(4)$ Å, $\beta = 107.04(1)^\circ$ (238 K). The results obtained by both ^{11}B and ^{13}C MAS NMR spectroscopy are discussed. Thermogravimetric studies under a flowing inert-gas atmosphere suggest that water, stemming from polycondensation of the hydrous borate species, is released from the clathrates at ca. 443 K (**1**) and 398 K (**2**) before the decomposition of the organic cations starts at ca. 603 K (**1**) and 603 K (**2**).

Key words: Pentaborate, boric acid, clathrate, diamond-related network, hydrogen bonding, tetrapropylammonium, tetrabutylammonium, crystal structure, ^{11}B MAS NMR, ^{13}C MAS NMR, thermogravimetry.

Supplementary Data relating to this article are deposited with the British Library as supplementary publication No. SUP 82172 (82 pages).

1. Introduction

In some clathrate systems the host components are linked by extensive hydrogen bonding into infinite, three-dimensional host networks. Examples are provided by

* Author for correspondence.

the classical host compounds water, urea, thiourea and hydroquinone. A very interesting recent development in this field of host–guest chemistry is the construction of new three-dimensional, very open hydrogen-bonded networks by self-assembly of appropriately designed molecules possessing tetrahedrally directed functional groups; see, for example, the diamond-related ('diamondoid') networks formed by some tetracarboxylic acids [1] or by some rigid tetrapyrindones [2] or the mixed diamondoid networks formed by cubane-like clusters $[M(CO)_3(\mu-OH)]_4$ ($M = Mn, Re$), which are tetrafunctional proton donors, and complementary difunctional proton-acceptor molecules like 1,2-diaminoethane [3]. Such extended open networks are capable of self-inclusion (i.e., interpenetration) and/or inclusion of molecular guest species.

It is of interest that in addition to the abovementioned *neutral* host frameworks, rather open hydrogen-bonded networks can also be formed by *anionic* species. For example, in the isotopic dipotassium and disodium salts of adamantane-1,3,5,7-tetracarboxylic acid four diamondoid structures of hydrogen-bonded dihydrogen tetracarboxylate anions interpenetrate each other, while the small alkali cations reside within helical channels [4]. Recently, we have shown that oligomeric hydrous pentaborate $[B_5O_6(OH)_4]^-$ ions are also capable of self-assembly into open hydrogen-bonded host frameworks, thus forming structurally related channel-type clathrates, $A[B_5O_6(OH)_4]$, with a number of differently-sized quaternary ammonium cations as guest species (e.g., $A = NMe_4^+, NEt_4^+, NPhMe_3^+$, piperidinium) [5].

We have extended our studies to the larger $N(nPr)_4^+$ and $N(nBu)_4^+$ ions and here report the preparation, crystal structures and thermal properties of the hydrous 'heptaborates' **1** and **2**. In particular we show that these compounds are also clathrates with isotopic porous hydrogen-bonded networks composed of $[B_5O_6(OH)_4]^-$ and $B(OH)_3$ species, and that there exists a relationship to the diamond net. Compounds **1** and **2** have previously been prepared and characterized by infrared spectroscopy and powder X-ray diffraction [6], yet the molecular structures of the hydrous borate species and the crystal structures remained undetermined.

2. Experimental

2.1. PREPARATION

Crystalline boric acid (Fluka, 99.5%), aqueous solutions of the respective tetraalkylammonium hydroxide [$N(nPr)_4OH$ (Fluka, 20%), $N(nBu)_4OH$ (Fluka, 40%)], and deionized water were used to prepare dilute solutions with the molar ratio $NR_4OH/B(OH)_3 = 1 : 7$. The solutions were slowly evaporated in a desiccator (over solid KOH) until crystals of **1** and **2** deposited. The crystals were recovered by filtration and dried in air. This method readily affords pure-phase material of **1** in the form of large colourless, transparent crystals with the shape of pseudo-hexagonal plates. In the case of **2**, which deposits in the form of colourless, transparent, needle-shaped crystals, care has to be taken to avoid simultaneous crystallization

of B(OH)₃. The products were recrystallized from deionized water and analysed by standard methods. *Anal. Found. (Calc. for NR₄[B₅O₆(OH)₄][B(OH)₃]₂):* **1** C, 27.4 (27.2); H, 7.2 (7.2); N, 2.7 (2.7)%; N : B = 1 : 7 (1 : 7). **2** C, 32.7 (32.8); H, 7.8 (7.9); N, 2.5 (2.4)%; N : B = 1 : 7 (1 : 7).

2.2. METHODS OF CHARACTERIZATION

Phase purity was checked at room temperature by powder X-ray diffraction (Guinier diffractometer, CuK_{α1} radiation). Additionally, variable-temperature powder X-ray photographs were taken on a Guinier camera.

A Netzsch STA 429 Thermoanalyzer was employed for simultaneous thermal analysis (STA) combining thermogravimetry (TG), derivative thermogravimetry (DTG) and differential thermal analysis (DTA): Flowing argon atmosphere, platinum crucible, sample weight 10–20 mg, heating rate 5 K min⁻¹. The STA studies were combined with mass spectrometric analysis using a Balzers QMG 511 apparatus.

Solid-state ¹¹B and ¹³C NMR spectra were recorded at room temperature on a Bruker MSL-400 spectrometer at 128.33 MHz and 100.83 MHz resonance frequency, respectively. Single-pulse excitation, magic angle spinning (MAS) and high-power proton decoupling were used for both nuclei, for the ¹³C spectra ¹H–¹³C cross-polarization (CP) was also applied. The spinning speeds were 15 kHz (¹¹B) and 8 kHz (¹³C). The chemical shifts of the ¹¹B and ¹³C nuclei are given relative to BF₃·OEt₂ and SiMe₄ (TMS), respectively.

2.3. SINGLE-CRYSTAL X-RAY STRUCTURE ANALYSES

Suitable crystals of **1** and **2** were enclosed in thin-walled glass capillaries and mounted on an Enraf-Nonius CAD4 diffractometer (graphite monochromator, MoK_α radiation, λ = 0.71073 Å). Intensities were measured by a variable ω/2θ-scan technique. Absorption effects were considered negligible.

The structures were solved by direct methods. Subsequent full-matrix least-squares refinements included the observed reflections which were weighted according to $w = 4F^2 / [\sigma_1^2 + (0.04F^2)^2]$. The function minimized was $\sum w(\Delta F)^2$. Approximate statistical occupancy factors of the disordered carbon atoms in **2** were derived from refinement and difference Fourier syntheses. Most hydrogen atoms, including all hydrogen atoms of the host frameworks, could be localized by difference Fourier methods. In the final cycles of refinement, the coordinates of the hydrogen atoms attached to the pentaborate anions and B(OH)₃ molecules were kept fixed as determined by difference Fourier synthesis. The hydrogen atoms of the alkyl groups were treated 'riding' on the carbon atoms assuming $d(\text{C-H}) = 0.99$ Å and tetrahedral bond angles [7]. No corrections were made for the well-known systematic error of X-ray methods to produce too short O–H and C–H bond lengths. Anisotropic and isotropic displacement parameters were used for the non-

TABLE I. $N(n\text{Pr})_4[\text{B}_5\text{O}_6(\text{OH})_4][\text{B}(\text{OH})_3]_2$ (1), $N(n\text{Bu})_4[\text{B}_5\text{O}_6(\text{OH})_4][\text{B}(\text{OH})_3]_2$ (2); crystal data and details of intensity measurement and structure refinement.

	1	2
Formula weight	528.18	584.30
Crystal size [mm]	$0.39 \times 0.30 \times 0.24$	$0.42 \times 0.30 \times 0.27$
Crystal system	monoclinic	monoclinic
Space group; Z	$P2_1/c$; 4	$P2_1/c$; 4
a [Å]	13.592(5)	13.874(3)
b [Å]	12.082(2)	12.585(1)
c [Å]	17.355(6)	17.588(4)
β [°]	106.60(2)	107.04(1)
V [Å ³]	2731.0(9)	2936.0(8)
T [K]	298	238
d_{calc} [M·m ³]	1.285	1.322
$F(000)$	1120	1248
$\mu(\text{MoK}\alpha)$ [mm ⁻¹]	0.103	0.102
Range of 2θ [°]	4–55	4–56
No. of reflections measured	6433	7340
No. of unique reflections	6150	7056
No. of observed reflections m ($I > 1.5\sigma_1$)	2643	4698
Refined parameters n	325	379
$R = \sum(\Delta F) / \sum F$	0.050	0.077
$R_w = \sum w(\Delta F)^2 / \sum wF^2$ ^{1/2}	0.051	0.079
$S = [\sum w(\Delta F)^2 / (m - n)]$ ^{1/2}	1.436	2.358
min, max $\Delta\rho$ [e Å ⁻³]	-0.22, +0.23	-0.39, +0.82 ^a

^a At close distance to atoms C(33) and C(34), indicating that some kind of disorder may be present which could not be modelled.

hydrogen and hydrogen atoms, respectively. Further details of the X-ray structure analyses are listed in Table I.

Computations were performed on a VAX3200 workstation using the Enraf-Nonius SDP program system [8]. Complex scattering factors for neutral atoms were taken from the International Tables for X-ray Crystallography [9]. Drawings were generated with the programs ORTEP [10] and SCHAKAL [11].

3. Results and Discussion

3.1. CRYSTAL STRUCTURES

Crystal data are listed in Table I, atomic parameters in Tables II and III, and selected interatomic distances and angles in Tables IV and V. Supplementary

TABLE II. N(nPr)₄[B₅O₆(OH)₄][B(OH)₃]₂ (1); fractional coordinates and equivalent isotropic displacement parameters U_{eq} [\AA^2] of the non-hydrogen atoms

Atom	x	y	z	100 U_{eq}^a
B(1)	0.2547(2)	0.0999(3)	0.2476(2)	3.28(7)
B(2)	0.2776(3)	0.2138(3)	0.3700(2)	3.66(8)
B(3)	0.3686(2)	0.0457(3)	0.3812(2)	3.53(8)
B(4)	0.2782(3)	0.1314(3)	0.1127(2)	3.71(8)
B(5)	0.1266(3)	0.0435(3)	0.1212(2)	3.66(8)
B(6)	0.5483(3)	0.2767(4)	0.2233(2)	5.6(1)
B(7)	0.0463(3)	0.4108(4)	0.2450(2)	5.7(1)
O(1)	0.2316(1)	0.1955(2)	0.2915(1)	3.89(4)
O(2)	0.3502(2)	0.1421(2)	0.4156(1)	4.44(5)
O(3)	0.3173(1)	0.0191(2)	0.30432(9)	3.62(4)
O(4)	0.3129(1)	0.1368(2)	0.19336(9)	3.91(5)
O(5)	0.1856(1)	0.0820(2)	0.0752(1)	4.32(5)
O(6)	0.1583(1)	0.0482(2)	0.20229(9)	3.82(4)
O(7)	0.2529(2)	0.3051(2)	0.4062(1)	5.18(5)
O(8)	0.4386(2)	-0.0264(2)	0.4260(1)	5.17(5)
O(9)	0.3343(2)	0.1746(2)	0.0667(1)	5.39(5)
O(10)	0.0334(2)	0.0000(2)	0.0828(1)	5.28(5)
O(11)	0.5056(2)	0.2916(2)	0.1435(1)	5.98(6)
O(12)	0.6318(2)	0.3342(2)	0.2643(1)	8.09(7)
O(13)	0.5098(2)	0.2041(2)	0.2662(1)	8.62(7)
O(14)	0.0771(2)	0.4091(2)	0.3267(1)	6.37(6)
O(15)	-0.0353(2)	0.4711(2)	0.2036(1)	7.50(6)
O(16)	0.0958(2)	0.3518(2)	0.2017(1)	8.37(7)
N	0.7804(2)	0.2118(2)	0.4939(1)	5.36(7)
C(11)	0.8789(2)	0.2380(3)	0.4725(2)	5.85(9)
C(12)	0.9641(3)	0.1556(4)	0.5010(2)	7.8(1)
C(13)	1.0520(3)	0.1838(4)	0.4675(2)	8.7(1)
C(21)	0.7391(3)	0.0990(3)	0.4616(2)	5.82(8)
C(22)	0.7324(3)	0.0782(3)	0.3744(2)	7.0(1)
C(23)	0.6807(3)	-0.0299(4)	0.3470(3)	10.5(1)
C(31)	0.7042(3)	0.3022(3)	0.4562(2)	6.33(9)
C(32)	0.6010(3)	0.2958(4)	0.4715(3)	8.6(1)
C(33)	0.5350(3)	0.3923(4)	0.4331(3)	10.9(1)
C(41)	0.7987(3)	0.2074(3)	0.5843(2)	7.2(1)
C(42)	0.8386(4)	0.3127(4)	0.6290(2)	10.1(1)
C(43)	0.8431(4)	0.3022(5)	0.7161(2)	12.3(2)

$$^a U_{eq} = (1/3) \sum_i \sum_j U_{ij} a_i^* a_j^* (\mathbf{a}_i \cdot \mathbf{a}_j).$$

TABLE III. $N(n\text{Bu})_4[\text{B}_5\text{O}_6(\text{OH})_4][\text{B}(\text{OH})_3]_2$ (2); fractional coordinates and equivalent isotropic displacement parameters U_{eq} [\AA^2] of the non-hydrogen atoms

Atom	<i>x</i>	<i>y</i>	<i>z</i>	100 U_{eq} ^a
B(1)	0.2586(2)	0.0905(2)	0.2461(2)	2.41(5)
B(2)	0.2715(2)	0.1968(3)	0.3680(2)	2.77(6)
B(3)	0.3717(2)	0.0418(3)	0.3786(2)	2.81(6)
B(4)	0.2720(2)	0.1370(2)	0.1122(2)	2.70(6)
B(5)	0.1303(2)	0.0389(2)	0.1209(2)	2.72(6)
B(6)	0.5506(2)	0.2678(3)	0.2142(2)	3.65(7)
B(7)	0.0182(3)	0.3641(3)	0.2495(2)	4.50(8)
O(1)	0.2287(1)	0.1784(1)	0.28957(9)	2.72(3)
O(2)	0.3475(1)	0.1322(2)	0.41290(9)	3.48(4)
O(3)	0.3251(1)	0.0161(1)	0.30158(9)	2.72(3)
O(4)	0.3121(1)	0.1335(1)	0.19216(9)	2.66(3)
O(5)	0.1820(1)	0.0876(2)	0.07494(9)	3.41(4)
O(6)	0.1668(1)	0.0341(1)	0.20077(9)	2.68(3)
O(7)	0.2389(1)	0.2780(2)	0.4050(1)	4.20(4)
O(8)	0.4421(1)	-0.0257(2)	0.4245(1)	4.32(4)
O(9)	0.3213(1)	0.1883(2)	0.0662(1)	4.15(4)
O(10)	0.0390(1)	-0.0063(2)	0.0826(1)	4.01(4)
O(11)	0.5017(2)	0.2920(2)	0.1370(1)	4.94(5)
O(12)	0.6382(2)	0.3172(2)	0.2538(1)	5.32(5)
O(13)	0.5163(2)	0.1933(2)	0.2550(1)	4.96(5)
O(14)	0.0583(2)	0.3770(2)	0.3301(1)	5.01(5)
O(15)	-0.0687(2)	0.4134(2)	0.2084(1)	5.69(5)
O(16)	0.0644(2)	0.3033(2)	0.2074(1)	6.51(6)
N	0.7500(2)	0.2461(2)	0.4963(1)	4.61(6)
C(11)	0.8446(2)	0.2680(3)	0.4734(2)	5.39(7)
C(12)	0.9317(3)	0.1988(4)	0.5149(2)	8.0(1)
C(13A) ^b	1.0384(8)	0.200(1)	0.5001(7)	7.5(3)
C(13B) ^c	1.0112(3)	0.2158(4)	0.4733(3)	5.6(1)
C(14A) ^b	1.039(1)	0.123(1)	0.4337(8)	10.3(4)
C(14B) ^c	1.0930(4)	0.1353(6)	0.5037(4)	9.9(2)
C(21)	0.7197(2)	0.1309(3)	0.4827(2)	4.98(7)
C(22)	0.7176(3)	0.0871(3)	0.4015(2)	7.0(1)
C(23)	0.6794(3)	-0.0230(3)	0.3897(2)	7.8(1)
C(24)	0.6853(3)	-0.0756(3)	0.3158(2)	8.4(1)
C(31)	0.6656(3)	0.3168(3)	0.4435(2)	6.31(9)
C(32)	0.5676(3)	0.3171(3)	0.4643(3)	7.7(1)
C(33)	0.4798(3)	0.3772(4)	0.4046(3)	9.2(1)
C(34)	0.5117(4)	0.4766(4)	0.3884(3)	11.0(2)
C(41)	0.7654(2)	0.2706(3)	0.5834(2)	5.13(7)
C(42)	0.7909(3)	0.3871(3)	0.6062(2)	7.3(1)
C(43)	0.7895(3)	0.4101(4)	0.6897(2)	8.1(1)
C(44)	0.8701(4)	0.3599(5)	0.7506(2)	10.9(2)

$$^a U_{\text{eq}} = (1/3) \sum_i \sum_j U_{ij} a_i^* a_j^* (\mathbf{a}_i \cdot \mathbf{a}_j).$$

^b Statistical occupancy factor 0.33 owing to disorder.

^c Statistical occupancy factor 0.67 owing to disorder.

TABLE IV. Bond lengths [Å] and angles [°] in pentaborate anions and boric acid molecules for **1** and **2**

	1	2		1	2
[B ₅ O ₆ (OH) ₄] ⁻ ion:					
B(1)–O(1)	1.466(3)	1.472(2)	O(1)–B(1)–O(3)	110.1(2)	110.7(1)
B(1)–O(3)	1.472(3)	1.466(2)	O(1)–B(1)–O(4)	109.3(2)	109.3(1)
B(1)–O(4)	1.461(3)	1.469(2)	O(1)–B(1)–O(6)	108.9(2)	108.2(1)
B(1)–O(6)	1.462(3)	1.472(2)	O(3)–B(1)–O(4)	108.5(2)	109.1(1)
			O(3)–B(1)–O(6)	109.5(2)	109.2(1)
			O(4)–B(1)–O(6)	110.5(2)	110.4(1)
			B(1)–O(1)–B(2)	123.4(2)	123.5(1)
			B(2)–O(2)–B(3)	118.4(2)	118.6(1)
			B(1)–O(3)–B(3)	122.5(2)	122.3(1)
			B(1)–O(4)–B(4)	124.2(2)	123.5(1)
			B(4)–O(5)–B(5)	118.9(2)	118.6(1)
			B(1)–O(6)–B(5)	123.3(2)	123.0(1)
B(2)–O(1)	1.345(3)	1.352(2)	O(1)–B(2)–O(2)	121.7(3)	121.1(2)
B(2)–O(2)	1.379(3)	1.381(2)	O(1)–B(2)–O(7)	119.8(3)	120.6(2)
B(2)–O(7)	1.358(3)	1.358(2)	O(2)–B(2)–O(7)	118.4(2)	118.3(1)
B(3)–O(2)	1.364(4)	1.375(2)	O(2)–B(3)–O(3)	121.7(2)	121.9(2)
B(3)–O(3)	1.356(3)	1.357(2)	O(2)–B(3)–O(8)	118.9(2)	118.6(1)
B(3)–O(8)	1.359(3)	1.365(2)	O(3)–B(3)–O(8)	119.4(3)	119.5(2)
B(4)–O(4)	1.346(3)	1.353(2)	O(4)–B(4)–O(5)	120.9(3)	121.3(2)
B(4)–O(5)	1.377(3)	1.377(2)	O(4)–B(4)–O(9)	120.3(3)	120.4(2)
B(4)–O(9)	1.355(3)	1.365(2)	O(5)–B(4)–O(9)	118.8(2)	118.3(1)
B(5)–O(5)	1.364(3)	1.372(2)	O(5)–B(5)–O(6)	121.9(2)	122.2(2)
B(5)–O(6)	1.351(3)	1.348(2)	O(5)–B(5)–O(10)	117.9(2)	117.6(1)
B(5)–O(10)	1.357(3)	1.372(2)	O(6)–B(5)–O(10)	120.2(3)	120.2(2)
B(OH) ₃ molecules:					
B(6)–O(11)	1.352(4)	1.364(2)	O(11)–B(6)–O(12)	121.5(3)	121.1(2)
B(6)–O(12)	1.347(4)	1.361(3)	O(11)–B(6)–O(13)	122.1(3)	122.3(2)
B(6)–O(13)	1.349(4)	1.349(3)	O(12)–B(6)–O(13)	116.4(3)	116.6(2)
B(7)–O(14)	1.359(4)	1.372(3)	O(14)–B(7)–O(15)	121.7(3)	121.5(2)
B(7)–O(15)	1.349(4)	1.360(3)	O(14)–B(7)–O(16)	121.2(3)	121.4(2)
B(7)–O(16)	1.348(4)	1.350(3)	O(15)–B(7)–O(16)	117.0(3)	117.1(2)

TABLE V. Donor-acceptor distances [Å] in hydrogen bonds O–H···O for **1** and **2**

	1	2		1	2
O(7)···O(9) ^{a,b}	2.699(2)	2.762(2)	O(10)···O(14) ^{a,b}	2.698(3)	2.747(2)
O(7)···O(14) ^a	2.703(3)	2.762(2)	O(12)···O(3) ^b	2.712(3)	2.788(2)
O(8)···O(8) ^{a,b}	2.709(3)	2.748(2)	O(13)···O(4)	2.737(3)	2.824(2)
O(8)···O(11) ^{a,b}	2.718(3)	2.745(2)	O(15)···O(6) ^b	2.809(3)	2.826(2)
O(9)···O(11) ^a	2.725(3)	2.773(2)	O(16)···O(1)	2.786(3)	2.798(2)
O(10)···O(10) ^{a,b}	2.755(3)	2.793(2)			

^a Hydrogen bond with twofold disordered hydrogen atom.

^b Acceptor atom is related by a symmetry operation to the corresponding position listed in Table II and III, respectively.

data available comprise atomic coordinates of hydrogen atoms, anisotropic displacement parameters, remaining interatomic distances and angles and structure factor amplitudes. The asymmetric unit of **1** and **2** contains one formula unit of $\text{NR}_4[\text{B}_5\text{O}_6(\text{OH})_4][\text{B}(\text{OH})_3]_2$, i.e., one tetraalkylammonium ion $[\text{N}(n\text{Pr})_4]^+$ or $[\text{N}(n\text{Bu})_4]^+$, one pentaborate $[\text{B}_5\text{O}_6(\text{OH})_4]^-$ ion, and two boric acid molecules. The molecular and ionic species generally possess typical geometrical parameters [5,12], yet some small deviations from maximum symmetries are observed (see below). The compounds can be favourably considered as clathrates with isotypic three-dimensional host structures composed of $[\text{B}_5\text{O}_6(\text{OH})_4]^-$ ions and $\text{B}(\text{OH})_3$ molecules which are linked via hydrogen bonds O–H···O. The cationic guest species NR_4^+ are trapped in the complex three-dimensional channel systems of the anionic host frameworks.

For a discussion of the host networks we first consider the pentaborate anions only. Each spirocyclic anion is composed of a central BO_4 tetrahedron sharing the four corners with BO_3 triangles to produce two almost planar six-membered B_3O_3 rings being at right angles with each other (Figure 1). Since the four terminal (exocyclic) hydroxyl groups, which can act both as proton donors and acceptors in hydrogen bonds, are arranged at the corners of an elongated tetrahedron the pentaborate anion constitutes a distorted tetrahedral building unit of maximum point group symmetry $\bar{4}2m(D_{2d})$ [13]. Therefore, such anions can be expected to be able to assemble into diamond-related networks by extensive hydrogen bonding via their four terminal OH groups. In fact, this is found in **1** and **2**. A distorted (i.e., along [102] elongated) diamondoid network of pentaborate anions is displayed in Figure 2 as an adamantane-like fragment, containing ten anions to one of which an additional anionic species is attached in order to illustrate the fourfold connectivity.

The considerable free intracrystalline space left by the anionic networks is partly filled with $\text{B}(\text{OH})_3$ molecules. Each planar acid molecule is located between two six-membered B_3O_3 rings of different $[\text{B}_5\text{O}_6(\text{OH})_4]^-$ ions and connected with these anions by pairwise hydrogen bonding in two $\text{B}_2\text{O}_4\text{H}_2$ rings (Figure 1).

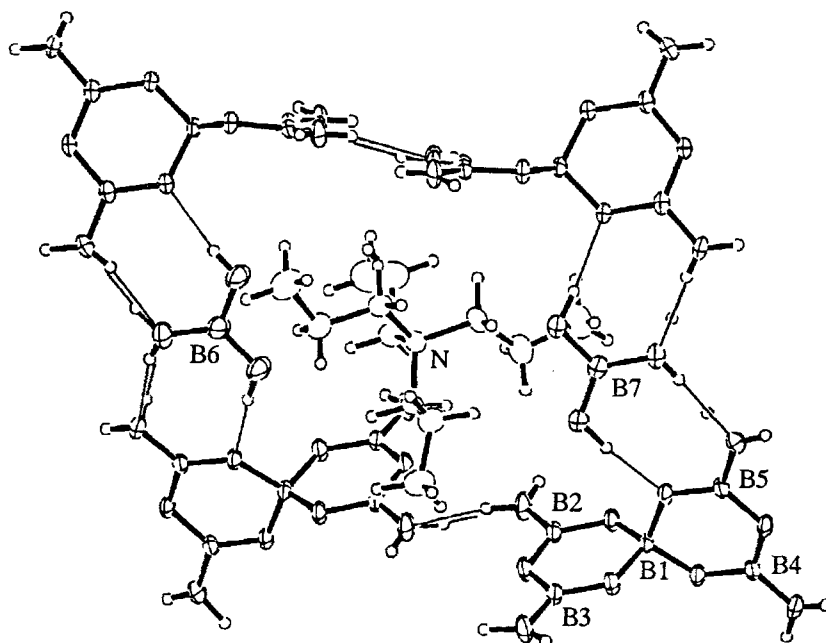


Fig. 1. ORTEP diagram illustrating the hydrogen bonding between the $[B_5O_6(OH)_4]^-$ and $B(OH)_3$ entities in the host framework of **1**; an $N(nPr)_4^+$ ion sitting with its central nitrogen atom in a side opening is also shown (see text). Numbering is given only for the boron and nitrogen atoms in the asymmetric unit; thick lines represent covalent bonds, thin lines represent $H \cdots O$ hydrogen bonds; the hydrogen atoms attached to the terminal O atoms of the anions and to one O atom of each $B(OH)_3$ molecule are twofold disordered.

Thereby, infinite buckled chains of alternating $B(OH)_3$ and $[B_5O_6(OH)_4]^-$ species are formed, pairs of which, in turn, are interconnected via hydrogen bonds (between pentaborate anions) into ribbons. Such buckled ribbons run, owing to the twist at the spiro-centers (by an angle of 90°), in two perpendicular directions through the crystal structure. Along the $[102]$ direction, which is parallel to the long (pseudo- $\bar{4}$) axis of the pentaborate anions, the ribbons follow each other in an ABCD sequence, i.e., successive parallel ribbons are in a staggered arrangement. Figure 3 displays a view of the structure of **1** parallel to the $[101]$ direction. In this direction channel-like voids occur that have free cross-sections of roughly $6.3 \times 2.5 \text{ \AA}$ in the case of **1** and $7.1 \times 3.2 \text{ \AA}$ in the case of **2**. These channels are interconnected with each other by side openings (Figure 1) to generate a three-dimensional pore system. The tetraalkylammonium cations sit with their central nitrogen atoms approximately in the centres of the side openings, while their alkyl chains protrude into the $[101]$ channels. The non-spherical shape of the cations is certainly the reason for the buckling of the acid molecule-anion ribbons in the host frameworks (see Figures 1

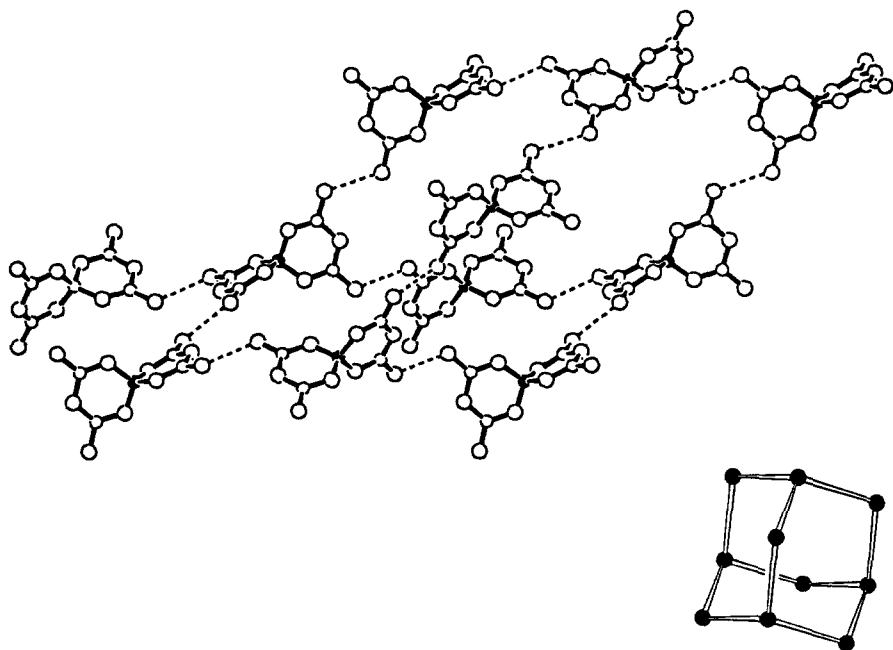


Fig. 2. Adamantane-like fragment cut out of the diamondoid network of hydrogen-bonded $[\text{B}_5\text{O}_6(\text{OH})_4]^-$ ions in **1**, with one additional anion attached in order to illustrate the fourfold connectivity. Donor–acceptor distances in $\text{O}-\text{H}\cdots\text{O}$ bonds are represented by dashed lines, hydrogen atoms are not shown. The central B(1) atoms of the anions in the adamantane-like fragment are drawn as black balls relating to the adamantane skeleton shown in the lower right corner.

and 3). The $\text{N}(n\text{Pr})_4^+$ ions are of the $\bar{4}2m(D_{2d})$ -type of conformer, the $\text{N}(n\text{Bu})_4^+$ ions belong to the $\bar{4}2m(D_{2d})$ -class of structures [14].

The difference in molecular volume of the $\text{N}(n\text{Pr})_4^+$ and $\text{N}(n\text{Bu})_4^+$ ions (V_m : 221 and 287 \AA^3 , respectively [15]) is clearly reflected in the hydrogen-bonding systems of the host structures, with considerably shorter, i.e., stronger, $\text{O}-\text{H}\cdots\text{O}$ bonds in **1** (mean $d(\text{O}\cdots\text{O}) = 2.732 \text{ \AA}$) than in **2** (mean $d(\text{O}\cdots\text{O}) = 2.779 \text{ \AA}$). On the other hand, the guest–host $\text{C}\cdots\text{O}$ distances ($\geq 3.216 \text{ \AA}$ in **1** and $\geq 3.244 \text{ \AA}$ in **2**) are typical for weak interactions. However, in **2** the $\gamma\text{-CH}_2$ and CH_3 groups of one butyl chain are disordered with occupancy factors for the two positions of 0.67 and 0.33, and there occur rather short interionic $\text{C}\cdots\text{C}$ guest–guest contacts down to 3.390 \AA (compared with $d(\text{C}\cdots\text{C}) \geq 3.778 \text{ \AA}$ in **1**). These facts indicate that the enclathration of the larger $\text{N}(n\text{Bu})_4^+$ ions in the host framework encounters some stereochemical difficulties, in accord with the observation made in the course of the preparation that pure-phase material of **2** is not easily obtained (see Section 2.1).

In both compounds the hydrogen atoms are distributed between two half-occupied positions in all those $\text{O}-\text{H}\cdots\text{O}$ bonds that exist between hydroxyl groups

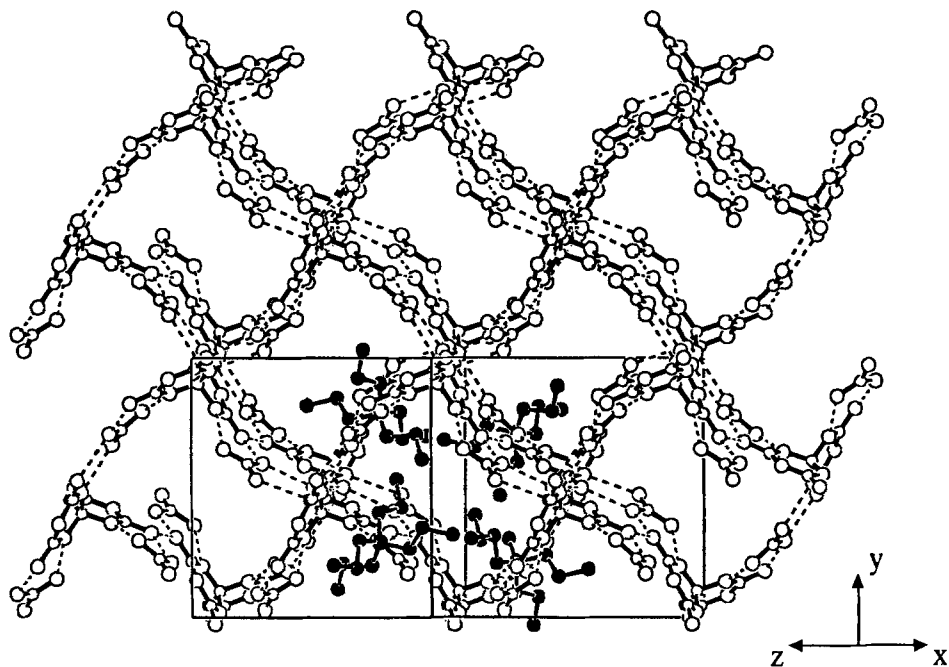


Fig. 3. Anionic host framework of **1** as viewed approximately along [101]. Some N(nPr)₄⁺ ions are also shown (black balls) in order to illustrate the location of the nitrogen atoms in the side openings and of the alkyl chains in the [101] channels.

of anions and/or B(OH)₃ molecules. Proton ordering occurs only in those hydrogen bonds that are accepted by endocyclic oxygen atoms of pentaborate anions (donors are OH groups of B(OH)₃ molecules). The latter hydrogen bonds possess generally the longest donor–acceptor distances in either structure.

3.2. MAS NMR STUDIES

The ¹¹B MAS NMR spectra of **1** and **2** are in accord with the molecular structures of the framework entities. The spectrum of **1** is shown in Figure 4. The sharp high-field line at 0.9 ppm originates from the (almost perfect) tetrahedral BO₄ unit of the pentaborate anions. The broad structured low-field feature consists of two component signals each with a quadrupolar line shape. These component signals are assignable to the axially symmetrical BO₃ groups in the [B₅O₆(OH)₄][−] and two B(OH)₃ species, respectively, which deviate slightly in their bond lengths and angles, and from ideal trigonal *6m2*(*D*_{3h}) symmetry (Table IV). In fact, good simulation of the whole spectrum has been obtained with three components (i) B(*sp*²), (ii) B'(*sp*²) and (iii) B(*sp*³) by assuming an intensity ratio (i) : (ii) : (iii) of 2 : 4 : 1. The spectral parameters [isotropic chemical shift (δ), quadrupole coupling constant (QCC), asymmetry parameter (η) of the electric-field-gradient

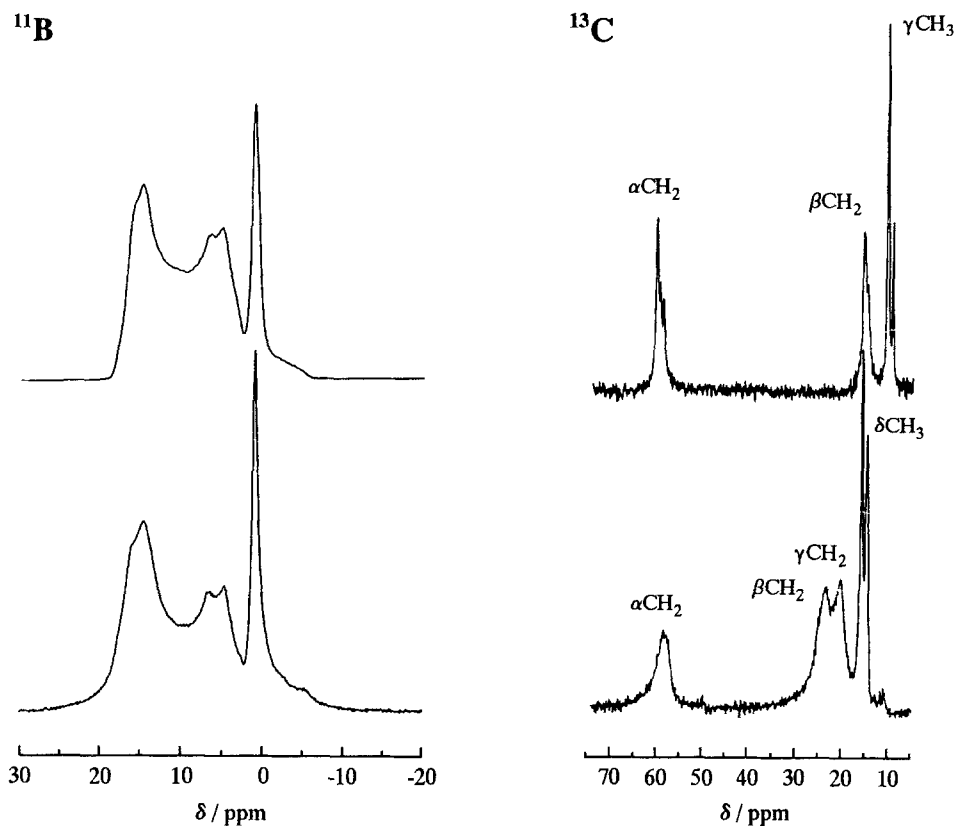


Fig. 4. Left-hand side: Experimental (bottom) and simulated (top) ^{11}B MAS NMR spectrum of **1**; spinning speed 15 kHz. Right-hand side: Experimental ^{13}C CP/MAS NMR spectra of **1** (top) and **2** (bottom); spinning speed 8 kHz.

tensor] obtained for **1** by simulation are as follows: (i) $\text{B}(sp^2)$; $\delta = 20.3$ ppm, $\text{QCC} = 2.47$ MHz, $\eta = 0.17$; (ii) $\text{B}'(sp^2)$; $\delta = 19.3$ ppm, $\text{QCC} = 2.54$ MHz, $\eta = 0.15$; (iii) $\text{B}(sp^3)$; $\delta = 0.9$ ppm, $\text{QCC} = 0.0$ MHz. These spectral parameters agree favourably with corresponding values that we have obtained recently for some pentaborate clathrates [5] and those that are reported in the literature [16].

From the ^{13}C CP/MAS NMR spectra shown in Figure 4 the following chemical shifts (δ/ppm) are obtained: **1** 60.1, 59.3, 58.6 ($\alpha\text{-CH}_2$), 15.7, 15.0 ($\beta\text{-CH}_2$), 10.7, 9.5 (CH_3); **2** 58.2 ($\alpha\text{-CH}_2$), 23.4 ($\beta\text{-CH}_2$), 20.1 ($\gamma\text{-CH}_2$), 15.6, 14.6 (CH_3). The shifts agree closely with values reported in the literature for $\text{N}(n\text{Pr})_4^+$ and $\text{N}(n\text{Bu})_4^+$ ions [17]. The considerable splittings seen for the resonance lines of the distinct CH_3 and CH_2 groups reflect the different local surroundings (guest–host and guest–guest interactions) of the single ^{13}C nuclei in the crystal structures. Similar line splittings have been observed for $\text{N}(n\text{Pr})_4^+$ and $\text{N}(n\text{Bu})_4^+$ ions occluded in zeolite-type materials [18].

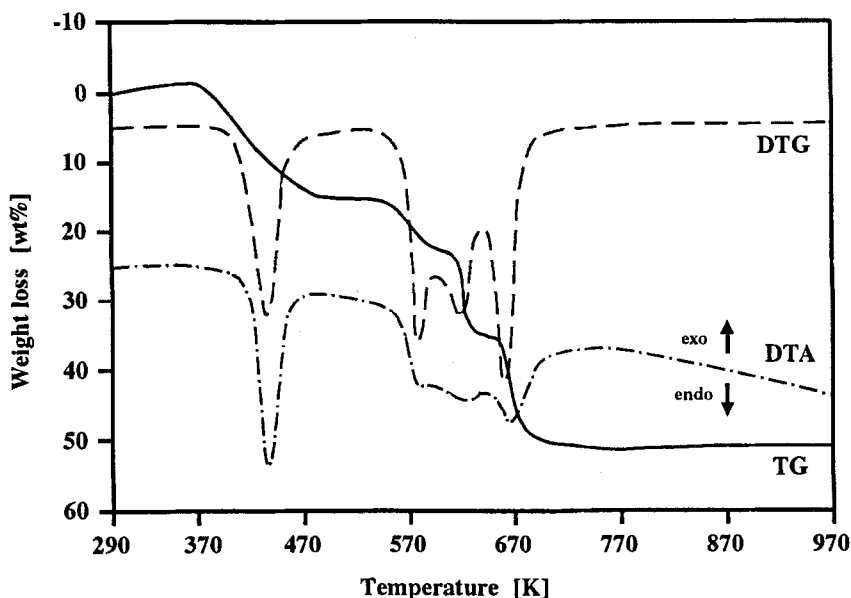
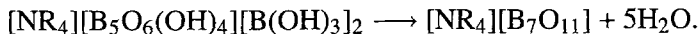


Fig. 5. Simultaneous thermal analyses curves for **1** measured in flowing argon.

3.3. THERMAL BEHAVIOUR

The simultaneous thermal analysis (TG/DTG/DTA) curves of **1**, measured under a flowing argon atmosphere, are shown in Figure 5. Similar curves have been obtained for **2**. The first endothermic decomposition reaction occurs at 443 and 398 K for **1** and **2**, respectively (the temperatures given correspond to the respective maxima in the DTG traces). Interestingly, the accompanying weight losses (exp.: 17.0% for **1**, 15.0% for **2**) agree nicely with the release of five H₂O molecules per formula unit (calc.: 17.1% for **1**, 15.4% for **2**) according to the polycondensation reaction:



That virtually only water is expelled during this first decomposition step is also suggested by simultaneous mass spectrometric analysis. At temperatures above 603 K (**1**) and 603 K (**2**), degradation of the organic cations takes place in several endothermic processes. The total weight losses (exp.: 54.0% for **1**, 58.0% for **2**) agree with those calculated for the release of all water and organic species (calc.: 53.9% for **1**, 58.3% for **2**); the final products exhibit a pale brown colour. Variable-temperature powder X-ray photographs reveal that the crystalline materials become amorphous already in the first decomposition (dehydration) step.

It is of interest that in **1** and **2** the polycondensation of the monomeric and oligomeric borate species via their hydroxyl groups, leading (ideally) from an extended hydrogen-bonded framework, $\left\{ \begin{smallmatrix} 3 \\ \infty \end{smallmatrix} \right\} [[\text{B}_5\text{O}_6(\text{OH})_4][\text{B}(\text{OH})_3]_2]$, to an anhydrous covalently-bonded framework, $\left\{ \begin{smallmatrix} 3 \\ \infty \end{smallmatrix} \right\} [\text{B}_7\text{O}_{11}]$, is almost completed before

decomposition of the organic cations starts. We have observed similar thermal behaviour for a number of pentaborate clathrates [5]. This suggests that the preparation of microporous anhydrous borates with occluded intact organic species may be possible under carefully controlled conditions of temperature. Since the pattern of hydrogen bonds in **1** and **2**, and also in the pentaborate clathrates [5], includes some endocyclic oxygen atoms of pentaborate anions at which condensation cannot take place, crystalline condensation products can only result after considerable structural rearrangement. Therefore, it is no surprise that we obtained only amorphous dehydration products by the simple temperature programs employed.

On the other hand, some natural and synthetic crystalline anhydrous borates with very open three-dimensional covalent frameworks are known, although being very scarce when compared with the many microporous aluminosilicate structures (zeolites). See, for example, the hilgardite group of minerals [19] and synthetic borates structurally related to them [20] and the two interpenetrating diamondoid frameworks in either phase of dimorphic $K[B_5O_8]$ [21]. Interestingly, the diamondoid frameworks of the latter compound consist of spiro-cyclic units that possess the same constitution as the pentaborate anions in **1** and **2**.

4. Conclusions

The results presented herein and in a preceding paper [5] demonstrate that oligomeric hydroxo(oxo)borate species can assemble into different open hydrogen-bonded network structures that are capable of enclathrating organic cations of various sizes and shapes, thus establishing a new, possibly extensive, class of clathrates. In particular, the diamondoid part of the pentaborate anions in the host frameworks of **1** and **2** suggests that even very open frameworks may be attainable. Additionally, in favourable cases it may also be possible to prepare microporous anhydrous borates from the hydrous borate clathrates via polycondensation.

References

1. a. O. Ermer: *J. Am. Chem. Soc.* **110**, 3747 (1988); b. O. Ermer and L. Lindenberg: *Helv. Chim. Acta* **74**, 825 (1991).
2. M. Simard, D. Su, and J.D. Wuest: *J. Am. Chem. Soc.* **113**, 4696 (1991).
3. a. S.B. Copp, S. Subramanian, and M.J. Zaworotko: *J. Am. Chem. Soc.* **114**, 8719 (1992); b. S.B. Copp, S. Subramanian, M.J. Zaworotko: *J. Chem. Soc., Chem. Commun.* 1078 (1993).
4. O. Ermer and L. Lindenberg: *Chem. Ber.* **123**, 1111 (1990).
5. M. Wiebcke, C.C. Freyhardt, J. Felsche, and G. Engelhardt: *Z. Naturforsch.* **48b**, 978 (1993).
6. G. Heller: *J. Inorg. Nucl. Chem.* **30**, 2743 (1968).
7. F.H. Allen: *Acta Crystallogr.* **B42**, 515 (1986).
8. *SDP – Structure Determination Package*, Enraf-Nonius, Delft, The Netherlands (1989).
9. *International Tables for X-ray Crystallography* Vol. IV, Kynoch Press, Birmingham (1974). Distributed by Kluwer Academic Publishers, Dordrecht, The Netherlands.
10. C.K. Johnson: *ORTEP II* Report ORNL-5138, Oak Ridge National Laboratory, TN, USA (1976).
11. E. Keller: *SCHAKAL92 – A FORTRAN Program for the Graphical Representation of Molecular and Crystallographic Models*, University of Freiburg (1992).
12. M. Gajhede, S. Larsen, and S. Rettrup: *Acta Crystallogr.* **B42**, 545 (1986).

13. A.F. Wells: *Structural Inorganic Chemistry* 5th Ed., Clarendon Press, Oxford, pp. 1072 (1984).
14. R.W. Alder, C.M. Maunder, and A.G. Orpen: *Tetrahedron Lett.* **31**, 6717 (1990).
15. a. D.M.P. Mingos and A.L. Rohl: *J. Chem. Soc., Dalton Trans.* 3419 (1991); b. A. Gavezzotti: *J. Am. Chem. Soc.* **103**, 5220 (1983).
16. a. G.L. Turner, K.A. Smith, R.J. Kirkpatrick, and E. Oldfield: *J. Magn. Reson.* **67**, 544 (1986); b. D. Müller, A.-R. Grimmer, U. Timper, G. Heller, M. Shakibaie-Moghadam: *Z. Anorg. Allg. Chem.* **619**, 1262 (1993).
17. G. Engelhardt and D. Michel: *High-Resolution Solid-State NMR of Silicates and Zeolites*, John Wiley & Sons, Chichester, p. 350 (1987).
18. a. J.-M. Chezeau, L. Delmotte, J.-L. Guth, and M. Souldard: *Zeolites* **9**, 78 (1989); b. N. Dumont, Z. Gabelica, E.G. Derouane, and L.B. McCusker: *Microporous Mater.* **1**, 149 (1993); c. J.B. Nagy, Z. Gabelica, and E.G. Derouane: *Zeolites* **3**, 43 (1983).
19. a. C. Wan and S. Ghose: *Am. Mineral.* **68**, 604 (1983); b. P.C. Burns and F.C. Hawthorne: *Acta Crystallogr.* **C50**, 653 (1994).
20. S. Menchetti, C. Sabelli, and R. Trosti-Ferroni: *Acta Crystallogr.* **B38**, 2987 (1982).
21. J. Krogh-Moe: *Acta Crystallogr.* **B28**, 168 (1972).